Click Here for Full Article

Tectonic inheritance and continental rift architecture: Numerical and analogue models of the East African Rift system

Giacomo Corti,[1] Jolante van Wijk,[2,3] Sierd Cloetingh,[4] and Chris K. Morley[5]

[1] The western branch of the East African Rift is composed of an arcuate succession of elongate asymmetric basins, which differ in terms of interaction geometry, fault architecture and kinematics, and patterns of uplift/subsidence and erosion/sedimentation. The basins are located within Proterozoic mobile belts at the edge of the strong Tanzanian craton; surface geology suggests that the geometry of these weak zones is an important parameter in controlling rift development and architecture, although other processes have been proposed. In this study, we use lithosphere-scale numerical models and crustal-scale analogue experiments to shed light on the relations between preexisting structures and rift architecture. Results illustrate that on a regional scale, rift localization within the mobile belts at the curved craton's western border results in an arcuate rift system, which implies that under a constant extensional stress field, part of the western branch experienced orthogonal extension and part oblique extension. Largest depocenters are predicted to form mostly orthogonal to the extension direction, and smaller depocenters will form along the oblique parts of the rift. The varying extension direction along the rift zone furthermore results in lengthwise varying rift asymmetry, segmentation characteristics, and border fault architecture (trend, length, and kinematics). Analogue models predict that discrete upper crustal fabrics may influence the location of accommodation zones and control the architecture of extension-related faults at a local scale. Models support that fabric reactivation is responsible for the oblique-slip kinematics on faults and for the development of Z-shaped or arcuate normal faults typically documented in nature. **Citation:** Corti, G., J. van Wijk, S. Cloetingh, and C. K. Morley (2007), Tectonic inheritance and continental rift architecture: Numerical and analogue models of the East African Rift system, *Tectonics*, *26*, TC6006, doi:10.1029/2006TC002086.

1. Introduction

[2] The western branch of the East African Rift (Figure 1) is considered an archetype of continental rifts at an early stage of development [e.g., *Rosendahl*, 1987]. The western branch is composed of a system of distinct segments that developed since the Miocene (circa 12–10 Ma) [e.g., *Ebinger*, 1989] within Proterozoic mobile belts at the western border of the mechanically strong Tanzanian craton [*McConnell*, 1969, 1972; *Morley*, 1988; *Ebinger*, 1989; *Versfelt and Rosendahl*, 1989; *Ring*, 1994; *Petit and Ebinger*, 2000; *Nyblade and Brazier*, 2002]. The rift system is composed of an arcuate series of elongate, deep sedimentary basins. The basins are typically 80 to 100 km long and up to 6–7 km deep [*Morley*, 1989]. Basin cross-sectional geometry is generally asymmetric half graben style, where the thickest basin fills, and greatest water depths, lie in the hanging walls of linear to arcuate border fault systems [*Rosendahl et al.*, 1986; *Ebinger et al.*, 1987; *Rosendahl*, 1987; *Morley*, 1988, 1989; *Ebinger*, 1989]. Many of the basins (particularly Lake Tanganyika), display along-strike alternating basin asymmetry as the location of the master fault switches from one side of the basin to the other. Normal fault characteristics vary along the length of the rift, including linear, arcuate or short en echelon fault traces arranged in different sectors of the rift, with the kinematics of single structures varying from pure dip slip to oblique slip (Figure 1). Cumulative crustal extension and crustal thinning of the rift basins are thought to be very limited ($\beta < 1.5$) [e.g., *Morley*, 1988, 1989; *Ebinger*, 1989; *Kusznir et al.*, 1995; *Karner et al.*, 2000].

[3] Linking and mechanical interaction between adjacent basins occurs across accommodation zones. These accommodation zones are structurally complex areas, where significant along-axis variations in subsidence of grabens and elevation of uplifted flanks occur [*Rosendahl*, 1987; *Morley et al.*, 1990]. In the western branch, the sparse volcanic activity coincides with accommodation zones [e.g., *Ebinger*, 1989]. The locations of eruptive centers are found to be related to faults [*Ebinger et al.*, 1989], and volcanic activity seems to begin during the initial stages of continental rift development [e.g., *Ebinger*, 1989].

[4] Previous studies have defined a range of different processes that might control the structural variability and along-axis segmentation of the rift system.

[5] 1. *Scholz and Contreras* [1998] suggested that variations in the mechanical properties of the rifting plate influence the length, width, and style of faults in East Africa.

[6] 2. Southward rift propagation is proposed to have contributed to the diachronous development of rift basins and differences in evolution between basins [*Ebinger et al.*, 1987;
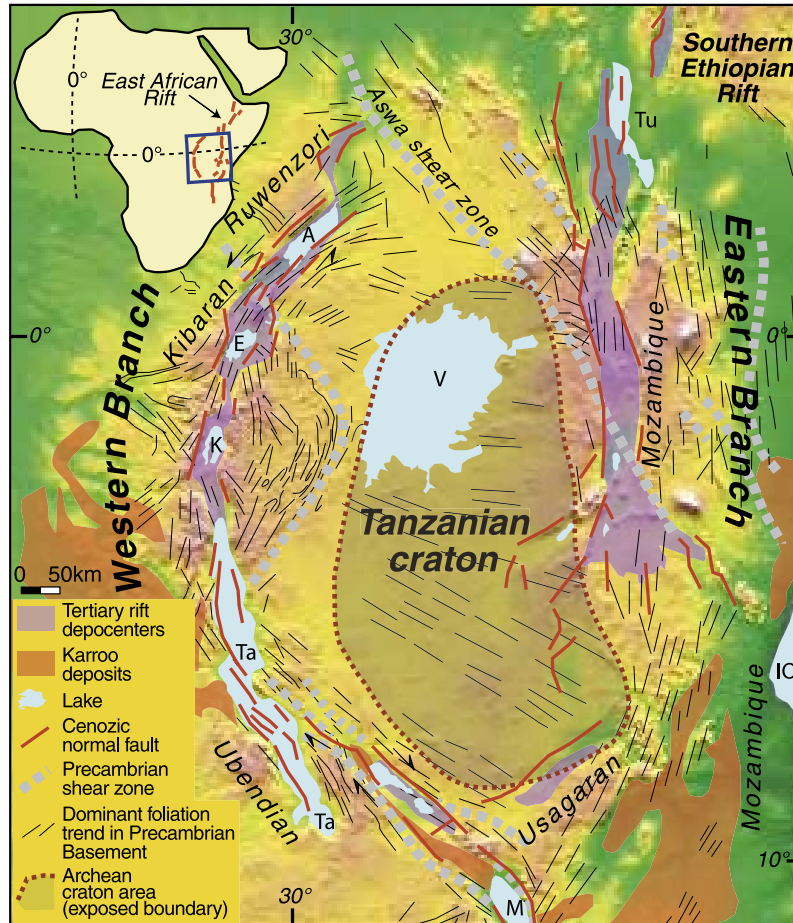
[1] Consiglio Nazionale Delle Ricerche–Istituto di Geoscienze e Georisorse, Unità Operativa di Firenze, Florence, Italy.
[2] Institute of Geophysics and Planetary Physics, Scripps Institution of Oceanography, La Jolla, California, USA.
[3] Now at Earth and Environmental Sciences Division, Los Alamos National Laboratory, Los Alamos, New Mexico, USA.
[4] Tectonics Department, Vrije Universiteit, Amsterdam, Netherlands.
[5] PTT Exploration and Production, Bangkok, Thailand.

Figure 1. Main structural features of the eastern and western branches of the East African Rift [after *Versfelt and Rosendahl*, 1989; *Morley*, 1999a; *Walker et al.*, 2004]. Rift zones follow old mobile belts and avoid the strong Tanzanian craton. A, Lake Albert; E, Lake Edward; K, Lake Kivu; IO, Indian Ocean; M, Lake Malawi; Ta, Lake Tanganyika; Tu, Lake Turkana; V, Lake Victoria.

Ebinger, 1989]. However, a southward age progression in the western branch is debated by *Nyblade and Brazier* [2002].

[7] 3. The segmentation of rift basins linked via accommodation zones is thought to be shaped by magmatic processes [*Ebinger et al.*, 1989].

[8] 4. *Delvaux et al.* [1992] and *Ring et al.* [1992] found indications for a change in stress orientation during discrete episodes of rifting in the Rukwa area and Malawi rift. *Ring et al.* [1992] determined that older faults at the outermost part of the rift have a different kinematic style than younger faults toward the center of the rift. Analogue modeling experiments show that such a distribution of fault kinematics can indeed be explained by a change in stress direction [e.g., *Corti et al.*, 2003].

[9] 5. A spatially periodic mantle anomaly along the length of the rift is proposed to cause the observed large-scale rift segmentation [*Ebinger et al.*, 1987]. *Ebinger et al.* [1987] developed this hypothesis to explain the inconsistent correlation between the trends of border fault segments and preexisting structures. However, other studies show that the nature of the prerift fabric, in combination with the orientation of the stress field, has influenced the Lake Tanganyika rift zone [e.g., *Versfelt and Rosendahl*, 1989; *Ring*, 1994] and can explain the seemingly inconsistent correlation between preexisting structures and fault patterns. The preexisting lithosphere structure and extension orientation are the focus of the present study.

[10] In this study, rift architecture and segmentation in relation to the geometry of the Tanzanian craton and the surrounding Proterozoic mobile belts are investigated through numerical and analogue models. The relationship between the tectonic inheritance and rifting is obvious on a continental scale, as normal faults localize within the mobile belts (Kibaran, Ubendian, Ruwenzori belts) at the craton's western edge [*McConnell*, 1969, 1972; *Versfelt and Rosendahl*, 1989; *Ring*, 1994]. However, on the local scale of individual rift basins or faults the relation with prerift structures is more enigmatic: While field works [e.g., *Lezzar et al.*, 2002] and previous analogue models [e.g., *Bellahsen and Daniel*, 2005; *Michon and Sokoutis*, 2005] suggest that preexisting upper crustal weakness may influence fault architecture and basin development, other studies have shown that structures may even cross ancient fabrics [e.g., *Ebinger*, 1989]. We test whether the preexisting structure

can explain the segmented character of the rift, or that other processes, such as diapiric magmatism, are needed. A modeling approach has been chosen in which analogue experiments on crustal scale are complemented by numerical viscoelastic models of lithosphere deformation.

2. Boundary Conditions of Deformation

[11] Rifting in East Africa has been attributed to the occurrence of one [e.g., *Ebinger and Sleep*, 1998] or two [e.g., *George et al.*, 1998] mantle plumes impinging the base of the lithosphere or, more recently, to a broader mantle upwelling (the African Superplume) connected to a lower mantle anomaly [e.g., *Benoit et al.*, 2006]. Huge amounts of volcanic rocks, uplift of large regions and subsequent deformation are the primary response to these active rifting settings, as observed in Kenya and Ethiopia. Conversely, in the western branch volcanism is scarce and limited uplift is localized to volcanic zones, suggesting that magma intrusion may be responsible for the local topography. Thus the impingement of a mantle plume on the lithosphere and the related doming are not the driving mechanism for rift development in the western branch. The eastward movement of the Somalia plate (or the Tanzanian craton) is most probably responsible for rifting in the area; consequently, in our experiments far field stresses determines the extensional deformation of the lithosphere.

[12] Extension is suggested to occur in an approximately E-W direction, as supported in nature by geological data [*Morley*, 1988, 1989; *Daly et al.*, 1989; *Ebinger*, 1989; *Lezzar et al.*, 2002], current seismicity [*Fairhead and Stuart*, 1982; *Bungum and Nnko*, 1984; *Shudofsky*, 1985; *Shudofsky et al.*, 1987; *Kebede and Kulhanek*, 1991; *Foster and Jackson*, 1998], GPS analysis [*Fernandes et al.*, 2004; *Calais et al.*, 2006] and analogue modeling results [*Michon and Sokoutis*, 2005].

[13] The velocity of extension is fixed at ~2 mm a^{-1}; similar low-extension velocities in the western branch are predicted on the basis of geological constraints [*Morley*, 1988; *Ebinger*, 1989], and supported by analysis of the Nubia-Somalia motion based on plate kinematics [*Jestin et al.*, 1984; *Lemaux et al.*, 2002], GPS data [*Fernandes et al.*, 2004], and current seismicity [*Foster and Jackson*, 1998]. Cumulative crustal stretching and thinning of the rift basins are thought to be very limited: Extension values ranging from ~6 to ~19 km are suggested by geological analysis [*Morley*, 1988, 1989; *Ebinger*, 1989], and mechanical and gravity modeling [*Kusznir et al.*, 1995; *Karner et al.*, 2000].

[14] Seismic analysis indicates the occurrence of many earthquakes of large magnitude in the deep crust [e.g., *Shudofsky*, 1985; *Shudofsky et al.*, 1987; *Jackson and Blenkinsop*, 1993; *Nyblade and Langston*, 1995; *Camelbeeck and Iranga*, 1996; *Foster and Jackson*, 1998]. Most of the deep earthquakes are localized at the extremities of the western branch, suggesting early stages of rift development in cold, strong continental crust where deep faults can traverse much of the crust [*Morley*, 1989; *Morley et al.*, 1999].

[15] The pervasive weaknesses that correspond to the curved geometry of the mobile belts at the boundary of the Tanzanian craton have been considered in both modeling approach. In the analogue models we have also reproduced discrete upper crustal fabrics, whose trend is based on field works suggesting reactivation of the NNE to NE trending fabrics (Kibaran and Ruwenzori belts) in the northern part of the rift, NW trending fabrics (Ubendian belt) in the southern part and both fabric directions in the central part [*McConnell*, 1969, 1972; *Versfelt and Rosendahl*, 1989; *Ring*, 1994; *Morley*, 1999a; *Walker et al.*, 2004].

3. Analogue Modeling

3.1. Experimental Setup, Material, and Scaling

[16] Crustal-scale analogue models were designed to analyze rift architecture and segmentation in relation to the geometry of the Proterozoic mobile belts surrounding the Tanzanian craton. The experiments were performed at the Tectonic Modeling Laboratory of the Consiglio Nazionale Delle Ricerche–Istituto di Geoscienze e Georisorse of Florence University (Italy), using a pure and simple shear deformation apparatus. The models, characterized by total dimensions of ~110 cm × ~25 cm × ~3.5 cm, consisted of a basal ductile layer made of a mixture of corundum sand and silicone (lower crust analogue) overlaid by a brittle upper crust analogue made of sieved Qz sand (Tables 1 and 2). The models were built over the metal base of the deformation apparatus; to avoid boundary effects, all the sides of models were unconfined. Extensional deformation was achieved through displacement of a basal thin acetate sheet fixed to a mobile wall that was driven by a stepper motor controlled by a central unit. Motion of the basal sheet induced a central velocity discontinuity (VD), whose displacement was transferred by viscous coupling at the base of the sand layer. The VD localized the extensional deformation within the overlying crust and reproduced the pervasive fabric corresponding to the weak zones at the craton's western border. The velocity of the acetate sheet was fixed at 5 cm h^{-1}; geometric and dynamic-kinematic similarity (achieved through comparison of dimensionless ratios relating gravitational stresses to differential stresses for brittle and ductile deformation; see Table 2) ensured that the models simulated extension of a ~35 km thick continental crust at a velocity of extension of ~2 mm a^{-1}, in E-W direction (Table 2). Model evolution was monitored through top-view photos taken at regular time intervals; after deformation, the models were soaked in water and then sectioned to observe the internal structures.

[17] The reference model (CRS21) was characterized by a homogenous crustal rheology, whereas in another model (CRS22) discrete zones of weakness in the upper crust were simulated. These weaknesses were created by the introduction of pieces of cardboard through the sand layer down to the top of the silicone layer [*Bellahsen and Daniel*, 2005]. The introduction and removal of the cardboard results in grain rearrangements, creating a zone of dilation; this zone obeys a Coulomb's frictional slip criterion and represents a zone of weakness because the coefficient of friction is lower than the internal friction of the undisturbed sand. The dip of these weakness zones was ~90°, their width was ~5 mm

Table 1. Characteristics of Experimental Materials

Composition	Density, kg m^{-3}	Angle of Peak Internal Friction	Cohesion, Pa	Power Law Parameters[a]
Brittle layer, dry quartz sand (>99% SiO$_2$) with a rounded grain shape and a grain size <250 μm	~1550	~40°	~65	
Ductile layer, mixture of silicone Mastic Rebondissante 29 + corundum sand (100:60; % weight)	~1600			n: 1.4 A: 3 × 10^{-7} Pa^{-n} s^{-1}

[a]Measured with a conicylindrical viscometer at room temperature (18°C ± 2°).

and their trend was varied to match the main Proterozoic belts.

3.2. Experimental Results

[18] Upon extension, normal faults bounding a subsiding depression localized above the basal VD (Figures 2 and 3). In the reference model (CRS21), the deformation pattern was primarily controlled by the curvilinear shape of the VD and the lateral variation in rift kinematics. In the central part of the model, linear normal faults and basins developed roughly perpendicular to the direction of extension (Figures 2a–2c); these faults displayed dominantly dip-slip kinematics. Approaching the lateral edges of the models, structures were oblique or highly oblique to the extension direction (Figures 2a–2c). There, conditions of oblique rifting resulted in relatively short, en echelon oblique-slip boundary faults [*Tron and Brun*, 1991]. The dip of boundary faults was higher, basins were narrower and subsidence was less pronounced than in the areas of orthogonal extension, as observed in previous modeling [*Michon and Sokoutis*, 2005]. As observed in the numerical experiments (see below), analysis of model cross sections showed that curvature of the rift system resulted in a typical basin asymmetry, with border fault locations and basin tilting alternating over the length of the rift (Figure 2d). Indeed, in these oblique rifting conditions, the rift zone follows the (oblique) VD orientation, but the single basins are individually oriented according to the extension direction. This results in an alternating rift asymmetry; the patterns of crustal thinning and topography are not symmetric around the rift axes of the major rift zones and change along axis over such a rift.

[19] Model CRS22 contained upper crustal zones of weakness intended to simulate the discrete fabrics in the brittle crust in nature. The preexisting fabrics were able to control the fault architecture at a local scale by modifying the fault geometry and kinematics (Figures 3–5). By including these inherited weakness zones a good fit of extension-related structures between model and nature was obtained, as discussed in the following section.

3.3. Comparison Between Analogue Models and Nature

[20] Comparison of Figures 3b and 3c highlights the resemblance in large-scale fault pattern between model CRS22 and the western branch. As observed in lakes George, Kivu, and northern Tanganyika, the central part of the model (in the region dominated by extension-orthogonal long, linear normal faults in the reference model) displays reactivation of NNE to NE trending preexisting weaknesses as normal faults slightly oblique to the general trend of the rift; these oblique faults locally influence the location of accommodation zones (Figures 3b, 3c, and 5). Reactivation of these oblique fabrics seems to determine local maximums in the width of the deformed zone in both nature and experiments (Figure 3d). In the portion of the model corresponding to the northern Lake Tanganyika in nature, NW trending fabrics were locally reactivated as oblique-slip dextral faults, consistent with structural documentations (Figure 4) [*Lezzar et al.*, 2002]. At the southern edge of the model, NW trending (Ubendian orientation) weaknesses were strongly reactivated; these reactivations locally suppressed the en echelon arrangement of border faults that typically arise in models of oblique rifting and gave rise to anomalously long faults, similarly to the Rukwa fault system (Figures 3 and 5) [*Morley*, 1999b; *Morley et al.*, 1999]. Both in model and nature, the large-scale kinematics of the fault zones documents a component of dextral oblique-slip, consistent with oblique rifting resulting

Table 2. Scaling Parameters for Brittle and Ductile Deformation[a]

	ρ_d, kg m^{-3}	ρ_b, kg m^{-3}	g, m s^{-2}	h_d, m	h_b, m	μ	τ_c, Pa	V, m s^{-1}	R_m[b]	R_s[c]
Models	1600	1550	9.81	1 × 10^{-2}	2.5 × 10^{-2}	0.8	65	1.4 × 10^{-5d}	1.6	1.1
Nature	2950	2700	9.81	1 × 10^{4}	2.5 × 10^{4}	0.6	60 × 10^{6}	~6.5 × 10^{-11e}	3.3	2.0

[a]Parameters are ρ_d, lower crust density, kg m^{-3}; ρ_b, upper crust density, kg m^{-3}; g, gravitational acceleration, m s^{-2}; hd, lower crust thickness, m; h_b, upper crust thickness, m; μ, coefficient of internal friction; τ_c, cohesive strength, Pa; V, extension rate, m s^{-1}.
[b]$R_m = \rho g h_d / (\sigma_1 - \sigma_3)_{viscous}$; the differential stress in the viscous layer has been calculated using flow equations for power law materials (see *Corti et al.* [2004] for details of parameters).
[c]$R_s = \rho g h_b / (\sigma_1 - \sigma_3)_{brittle}$; the differential stress in the brittle layer has been calculated using governing equation for tensional faulting in Coulombian materials (see *Corti et al.* [2004] for details of parameters).
[d]Corresponding to 5 cm h^{-1} and a strain rate of ~7 × 10^{-5} s^{-1}.
[e]Corresponding to ~2 mm a^{-1} and a strain rate of ~3 × 10^{-16} s^{-1}.
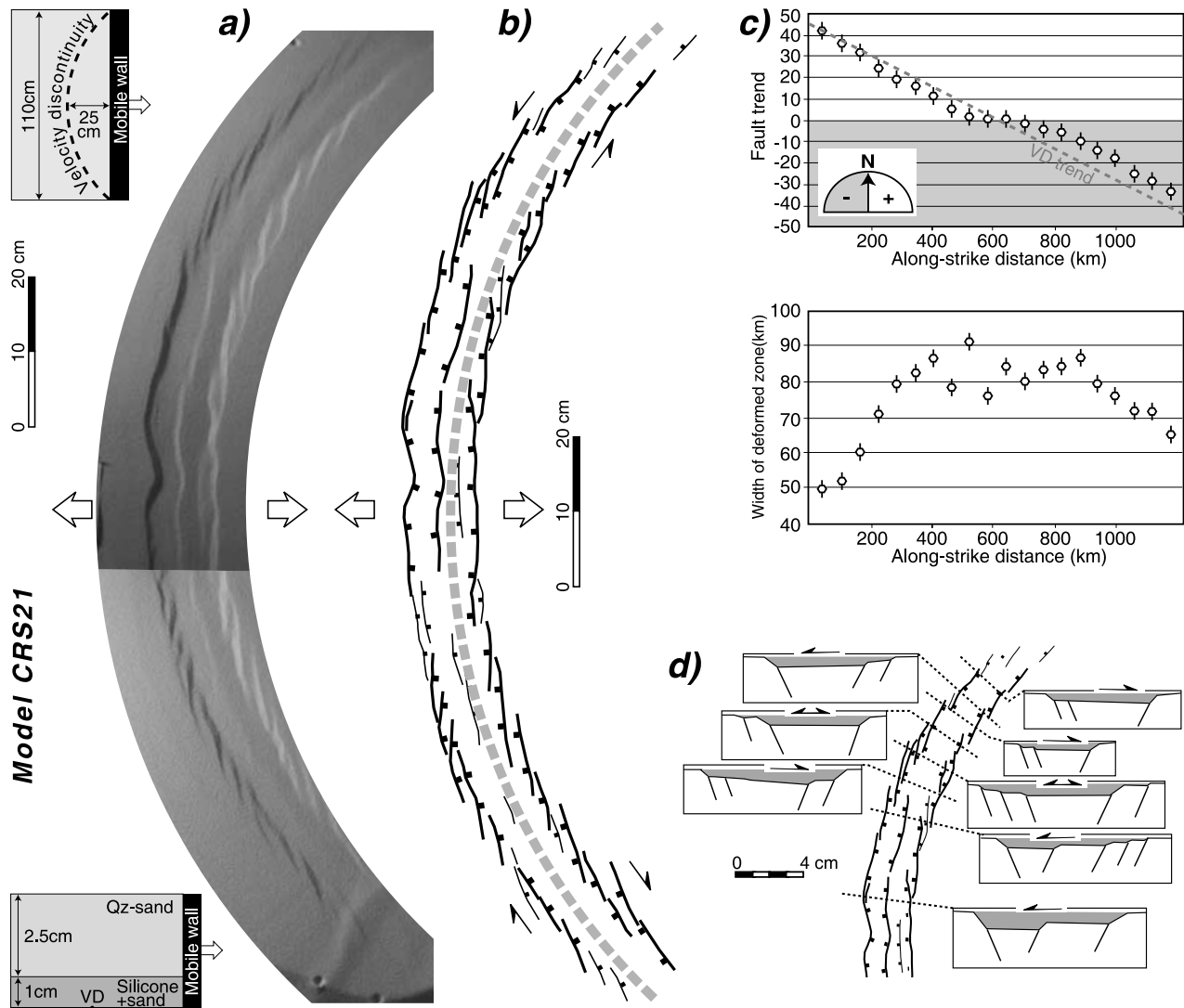
Figure 2. Results of analogue model CRS21 (with homogenous upper crust). (a) Top-view photo for 1 cm (=10 km in nature) of extension. Top inset shows the geometrical boundary conditions and bottom inset shows the rheological layering of the model. VD, velocity discontinuity. (b) Line drawing of structures in the model. (c) Graphs fault trend and basin width versus distance along the rift axis. (d) Schematic cross sections of the model. Only a representative portion of the models is illustrated.

from fabric reactivation under E-W extension [e.g., *Morley et al.*, 1999]. Although previous works suggested that the dextral kinematics on NW trending faults in the Lake Rukwa region may result from a pure strike-slip deformation along a right-lateral intracontinental transform zone [e.g., *Chorowitz*, 2005, and reference therein], the current modeling supports that the fault pattern and kinematics are more consistent with oblique extension at angle of ~40°–45° (Figure 5), a result which is compatible with fault architecture in nature [e.g., *Morley*, 1999a; *Morley et al.*, 1999]. Thus the dominant structural framework is set up

during oblique extension, whereas some minor structures (such as the minor folds or inversion features documented in nature but not observed in the models) may be explained as late features related to a change in regional stress [e.g., *Morley et al.*, 1999], as suggested by field work [e.g., *Delvaux et al.*, 1992; *Ring et al.*, 1992].

[21] Besides the local reactivation of weakness zones, boundary fault segments developing perpendicular to the extension direction and crossing the inherited upper crustal fabric are widely observed along the entire length of both the model rift and the western branch [e.g., *Ebinger*, 1989;
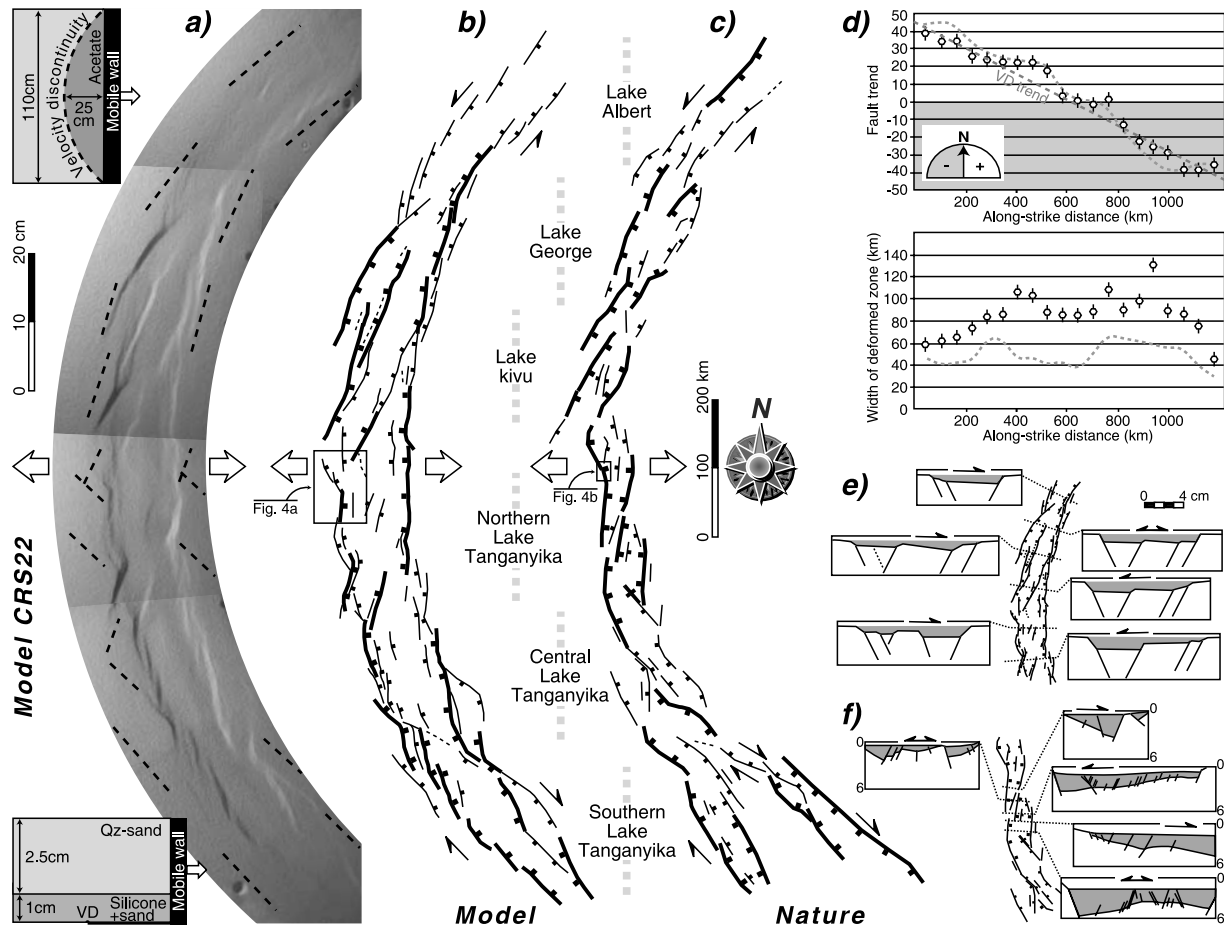
Figure 3. Results of analogue model CRS22 (with preexisting weakness zones). (a) Top-view photo of model CRS22 for 1 cm (=10 km in nature) of extension. Dashed lines on the model surface indicate the trend of nearly vertical preexisting zones of weakness reproduced inside the brittle layer. Insets and symbols are as in Figure 2. (b) Line drawing of structures in the model. (c) Drawing of fault pattern in nature [after *Morley*, 1988; *Ebinger*, 1989]. Note the transcurrent component of movement on faults and the Z-shaped or arcuate geometry of structures in both model and nature (see text for details). (d) Graphs of fault trend and width of the deformed zone versus distance along the rift axis for the model (hexagons with error bars) and nature (dotted line). Note the good correspondence in fault pattern; also note that local maximums in the width of the deformed zone in both nature and experiments occur in areas characterized by strong reactivation of oblique fabrics. (e) Schematic cross sections of the model; arrow indicate the sense of basin tilting. (f) Seismic lines in Lake Tanganyika [*Morley*, 1988]. Numbers refer to two-way traveltime. A similar asymmetry in boundary faults and basin tilting along the length of the rift is observed in both models and nature.

Morley, 1999a]. The interaction between these boundary fault segments and the reactivated structures creates sigmoidal or arcuate normal faults (see Figure 3, Lake Tanganyika area, and Figure 4), typically documented in the western branch of the EAR [*Rosendahl*, 1987; *Ebinger*, 1989; *Le Turdu et al.*, 1999; *Morley*, 1999a; *Lezzar et al.*, 2002].

[22]   As in the reference model, a typical basin asymmetry results from the analysis of model cross section; the pattern of alternating border faults and basin tilting strikingly resembles that characterizing Lake Tanganyika (Figures 3e and 3f).

[23]   Overall, the above results suggest that the large-scale rift architecture is compatible with the weakness zone

reactivation under a main phase of approximately E-W extension, although local fault pattern, focal mechanisms and stress orientations from the world stress map document more complex structural scenarios. For instance, in the Rukwa area an almost pure dip-slip kinematics on some faults is documented by focal mechanism solutions [e.g., *Foster and Jackson*, 1998] and field data [*Delvaux*, 2001], whereas the models predict a dominance of dextral oblique slip. These discrepancies may arise from a more complex accommodation of the distributed continental deformation in nature where slip partitioning between different set of structures [e.g., *Foster and Jackson*, 1998] and/or rapid switching between different paleostress environments
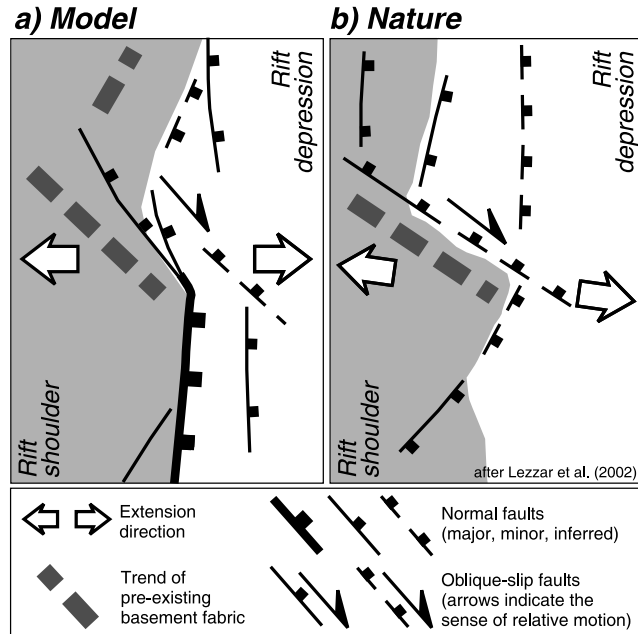
Figure 4. Comparison of arrangement and kinematics of transversal faults in Lake Tanganyika region in (a) model and (b) nature [after *Lezzar et al.*, 2002].

through time may occur [e.g., *Morley et al.*, 1999]. Another alternative is that local stress alignment in the oblique zones (e.g., S_{hmax} subparallel to fault orientation) is significantly different from the regional stress direction, as observed in the North Sea, for example [*Yale et al.*, 1994]. In addition, the counterclockwise rotation of the Tanzanian craton may contribute to the observed complex structural pattern [*Calais et al.*, 2006]. Obviously, the experimental results cannot explain all the structural details and the complexity characterizing natural rifts.

4. Numerical Experiments

[24] Numerical experiments were performed with the academic code Tecton [*Melosh and Raefsky*, 1980], which was coupled to a thermal routine [*Greenough and Robinson*, 2000]. The version included temperature-dependent power law rheology and buoyancy forces (for a more complete description, see *van Wijk and Blackman* [2005]). These numerical routines are widely used in studies of lithosphere deformation [*Furlong et al.*, 2001; *Govers and Wortel*, 2005]. We adopted a finite element modeling approach in which the model domain represented a lateral portion of lithosphere of 800×1000 km (Figure 6), and solved for thermal evolution and viscoelastic deformation of the lithosphere. The main simplifying assumption is that brittle behavior is not included in the model; a simple parameterization was used in which the value of the yield stress was given by the power law breakdown stress [*Tsenn and Carter*, 1987] and Byerlee's law was adopted in the upper crust. These viscoelastic lithospheric-scale numerical

experiments were preformed to complement the brittle, crustal-scale analogue modeling results.

4.1. Characteristics of the Modeling Setup

[25] A nonequidistant finite element grid was used; the node distance was smallest in the weak zone and crustal layers (~4 km) and coarser away from the weak zone and in the mantle layer. The grid followed the curvature of the prescribed weak zone (Figure 6a, only some of the grid lines are shown). A weak zone was included in the model to represent the Proterozoic mobile belt west of the Tanzanian craton where extensional deformation has localized. The weak zone followed the curved shape of the western side of the craton in these models; it is analogous to the VD the analogue models (see above). The width of this zone varied between the scaled equivalent of 50 and 200 km in different experiments, and was prescribed in the setup of the models as a zone with increased crustal thickness (that varies between experiments). For testing cases in which the strength difference between the weak zone and surrounding lithosphere is large, elastic parameters of the weak zone crust were lowered with a maximum of one order of magnitude. Apart from varying the relative weakness of the Proterozoic belt, a series of models were performed in which the curved shape of the craton was varied (Figure 6). Previous studies [*van Wijk*, 2005] have pointed out that these factors may control rift segmentation. The craton was included in the models as "normal" continental lithosphere instead of thick and cold lithosphere; this simplification is considered acceptable because the focus in these tests was on localization of deformation within the weak zone.

[26] In the experiments (Figure 6a), a setup was used in which the 125 km thick lithosphere was layered; a 35 km thick continental crust with a quartz-diorite composition overlays mantle with an olivine composition (Table 3). Lithosphere extension was simulated by pulling the left and right sides of the model domain approximately E-W whereby the extension velocity was held constant at 2 mm a^{-1}. The base of the domain was held horizontal but was free to move laterally, while the front and back sides and surface were free to move. Temperature boundary conditions included a constant normal mantle temperature at the base (1300°C) and top surface (0°C) and zero heat flow through the sides.

4.2. Results of Numerical Experiments

[27] Upon extension, deformation of the lithosphere localized in the prescribed weak mobile belt. The crust was thinned, and either a single, or a series of sedimentary basins were formed in the weak zone, depending on the curvature and relative weakness of the weak zone. The model predicted some upwelling of mantle material and slightly elevated temperatures beneath the rift basins (Figure 6b). For a sufficiently large strength contrast between the weak zone and surrounding lithosphere the model produced a series of rift zones (Figure 6c). Where the weak zone is oriented orthogonal to the extension direction a major sedimentary basin was formed; to the north and south of this basin, where rifting is oblique, crustal thinning was
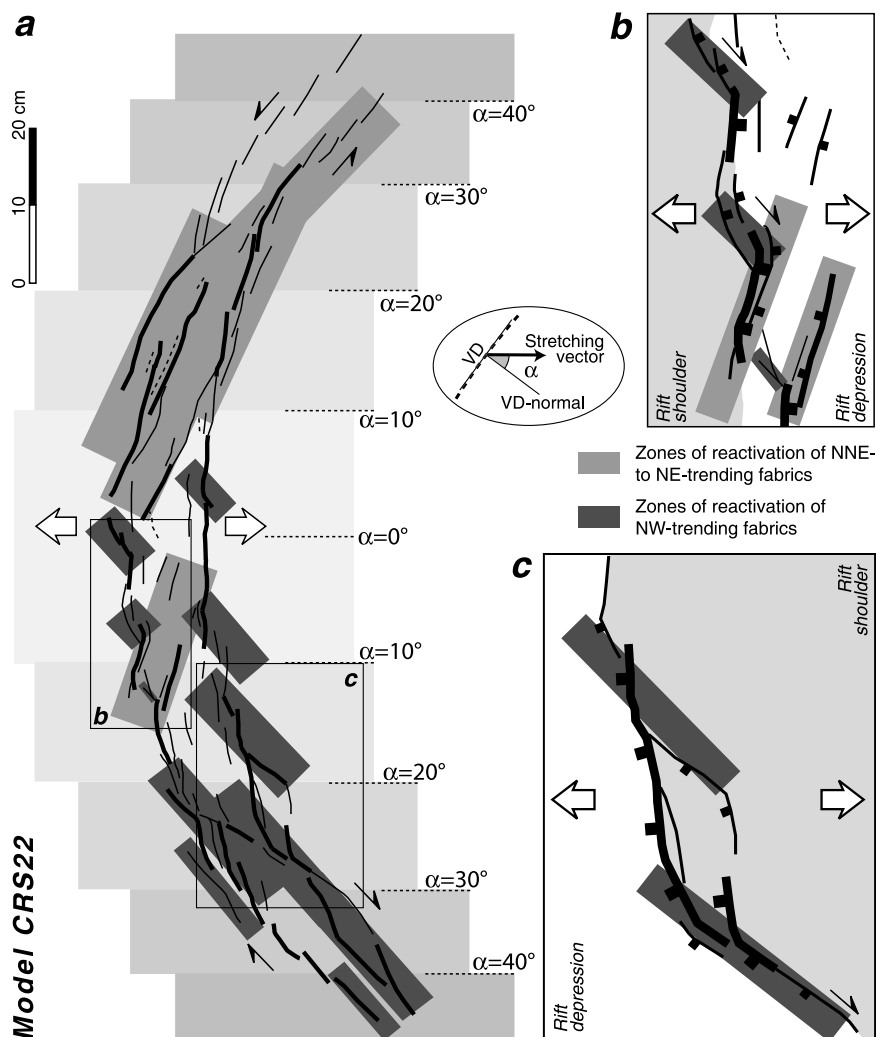
Figure 5. (a) Top-view photo of model CRS21 for 1 cm (=10 km in nature) of extension. Red and green dashed areas on the model surface indicate zones of reactivations of NW trending and NNE to NE trending preexisting zones of weakness, respectively. Light color fields indicate the different obliquity angle α (calculation shown in the small inset) in different parts of the model. Other symbols and panels are as in Figure 2. (b) Line drawing of structures in the model with indicated the areas of strong reactivation of NW trending (red pattern) and NNE to NE trending (green pattern) fabrics. (c–d) Details of the fault pattern showing the complex geometry of single faults resulting from interaction between extension-orthogonal fault segments and reactivated structures.

less pronounced and smaller rift basins were generated (Figure 6). The largest depocenter should be located orthogonal to the extension direction. In the case where a series of rift basins is formed, the smaller basins were somewhat rotated with respect to the weak zone; their orientation was clearly influenced by the extension direction. The origin of the strain localizations in the rift axis resulted from the strength difference between the weak zone and surrounding lithosphere. When lithospheric material in the weak zone is substantially weaker than the surrounding strong plate, stresses rotate between these materials, and multiple areas of localization that are somewhat rotated with respect to the orientation of the weak zone, are formed [*van Wijk and Blackman*, 2007]. The group of rift basins, however, follows the weak zone in

the lithosphere on a regional scale. When the strength difference between the weak mobile belt and surrounding lithosphere is small (case III), one sedimentary basin is formed upon extension (Figure 6c). Crustal thinning factors vary in this case over the length of the rift, and maximum crustal thinning is predicted in the area that is (almost) orthogonal to the extension direction, however, a segmented structure is no longer found.

[28] Whether structural segmentation will occur upon oblique extension of the lithosphere is thus dependent on the relative strength difference between weak zone and surrounding lithosphere in these numerical experiments, and on the relative orientation of the weak zone and the extension direction. In case II, where the curvature is limited
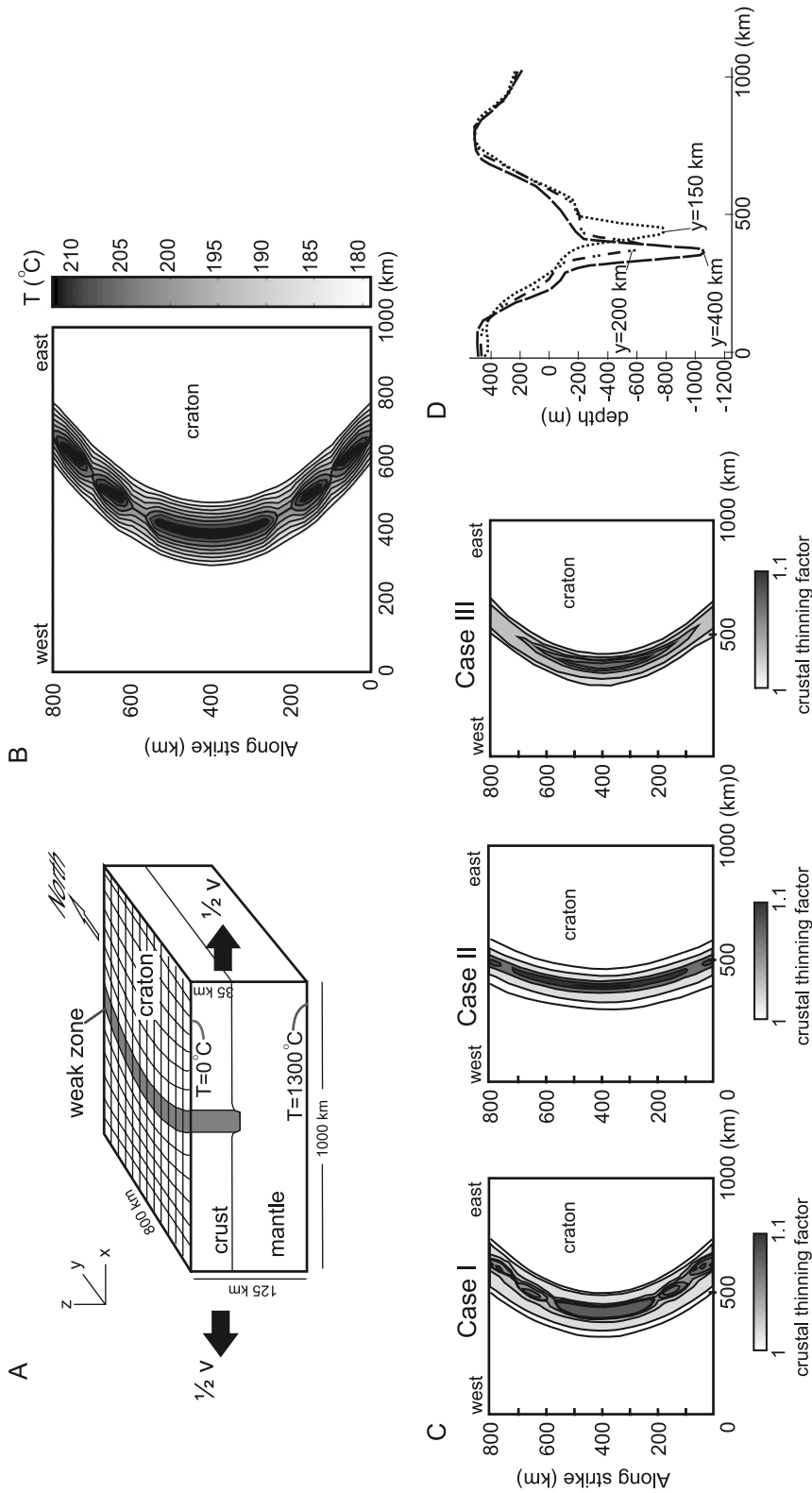
Figure 6. (a) Setup that is used for the numerical experiments. Relative strength, curvature, and with of weak zone (grey area) vary between experiments. The grid lines show how the grid deforms with the weak zone curvature (not all grid lines are shown). The lithosphere is extended by pulling the left and right sides (approximately E-W) with a constant total extension velocity of 2 mm a^{-1}. (b) Plan view of temperature structure for case I, in the upper crust. No significant thermal segmentation is present. (c) Case I, weak, 200 km wide weak zone, with crustal root extending to 43 km, and Young's modulus 1×10^{10} Pa. Crustal thinning is shown in plan view of model domain. Crustal thinning is the ratio between the initial crustal thickness and its present thickness. Case II, less curved weak zone, crustal root to 43 km depth, and Young's modulus 5×10^{10} Pa. Case III, curved weak zone (but with very small strength difference), the crustal root extending to 36 km depth, and Young's modulus 5×10^{10}. (d) Surface topography at three different places in the model for case I shown in Figure 6c. Note the deep main orthogonal basin (at y = 400 km), the less deep oblique basin (at y = 150 km), and the small amount of surface depression at y = 200 km that is in between the major rift zones.

Table 3. Thermal and Compositional Parameters Used in Numerical Experiments[a]

	Upper Crust	Lower Crust	Mantle Lithosphere
Density, kg m^{-3}	2700	2800	3300
Young's modulus, Pa	5×10^{10}	5×10^{10}	1×10^{10}
Poisson's ratio	0.25	0.25	0.25
Power law exponent n	3.0	3.0	3.0
Activation energy Q, kJ mol^{-1}	219	219	555
Material constant A, Pa^{-n} s^{-1}	5×10^{-18}	5×10^{-18}	7×10^{-14}
Conductivity, W m^{-1} K^{-1}	2.4	2.4	3.0
Specific heat, J kg^{-1} K^{-1}	1050	1050	1050
Thermal expansion, K^{-1}	1×10^{-5}	1×10^{-5}	1×10^{-5}
Heat production, W m^{-3}	1×10^{-6}	1×10^{-6}	-

[a]See *Kirby and Kronenberg* [1987] and *Turcotte and Schubert* [2002].

and most extension is orthogonal or suborthogonal, the experiments show formation of an elongated rift that follows the weak zone. Two smaller basins can be recognized to the north and south of this rift where the curvature of the prescribed weak zone is stronger.

[29] There is no significant thermal segmentation predicted at these low-extension and crustal thinning factors (Figure 6b). Temperatures vary only ~5–10°C between the warmest center of a segment and the places in between segments, and temperatures are too low everywhere for decompressional partial melting to occur. With ongoing extension and crustal thinning beyond what is observed at the western branch, the results show that in the case of a segmented rift, thermal segmentation is increased. Therefore we conclude that the segments are generally preferred zones for mantle upwelling and eventually decompression melting, although in the western branch such thermal segmentation following a passive rift model is not pronounced at the moment. The models furthermore predict that surface heat flow values in the rift are hardly elevated following about 10 km of extension (values about 8 mW m^{-2} higher than surrounding lithosphere). This reflects the limited thermal effect that we find after the crust has been thinned only slightly. We note, however, that processes such as magma migration and injection are not included in the model; these processes may locally increase surface heat flow values significantly.

4.3. Comparison Between Numerical Models and Nature

[30] Under the conditions discussed above, one of the findings of the numerical experiments is that the models predict, independent of relative strength differences between the weak zone and surrounding lithosphere, the formation of major depocenters in orthogonally rifted areas. All the cases investigated predict that the most prominent extensional deformation occurs in the orthogonal parts of the rifts and lateral along-strike variations in crustal thinning. However, development of distinct rift segments in the western branch best matches the finite element models where a relatively large prerift strength difference existed between the weak zones and adjacent lithosphere. With the assumption that the

extension direction is approximately E-W, the numerical models predict that Tanganyika rift would be the most prominent basin, as this basin is located approximately orthogonal to the extension direction. Estimates of sediment thickness at Lake Tanganyika are at least 4–5 km according to *Rosendahl et al.* [1992], while, for example, maximum sediment thickness of the Albertine rift, northern western branch [*Karner et al.*, 2000] are estimated to be up to 4.6 km, and Lake Kivu about 0.5 km [*Degens et al.*, 1973]. Although the numerical models apparently fail to explain why the Lake Albert rift has similar sediment thicknesses as Tanganyika rift, while the Lake Kivu rift is clearly less developed, there are actually a number of mitigating factors. First, Lake Albert may well fit the predictions of the model and have a thickness of Cenozoic sediments plus present-day lake depth of 2–3 km versus 5.5–6.5 km for Lake Tanganyika. The present maximum water depth for Lake Albert is only 58 m while it is about 1.5 km for Lake Tanganyika. This implies a significant difference in relatively recent subsidence rate or a major difference in sediment supply. In publicity material for oil exploration produced by the Ugandan National Oil Company, it is proposed that about half the sediment fill of Lake Albert is Mesozoic, with the Cenozoic section is only about 2–3 km thick. The 16 km extension proposed by *Karner et al.* [2000] seems too high for the Cenozoic alone, but it is more plausible if older rifts have been reactivated. Lake Albert may be similar to the other oblique trend in the western branch associated with Lake Rukwa, where Cretaceous and Karroo trends underlie Cenozoic sediments [*Roberts et al.*, 2004]. Recent vertebrate fossil discoveries indicate that the lower part of the Red Sandstone Group in the Rukwa rift is of Cretaceous age [*Krause et al.*, 2003, *O'Connor et al.*, 2006]. Consequently out of ~10km thickness of sedimentary rock (Karroo, Cretaceous and Tertiary) [*Morley et al.*, 1999] only a maximum of ~4 km maybe of late Tertiary age. Just like Lake Albert, the water depth (maximum of ~16 m) is significantly less than Lake Tanganyika. Consequently maximum subsidence in the Lake Albert and Lake Rukwa rifts appears to be some 50–70% of subsidence in Lake Tanganyika.

[31] Lake Kivu cannot easily be compared with the other rifts because of the major impact of igneous activity. The total thickness of basin fill (sediment plus volcanics plus volcaniclastics) is unknown because the seismic data did not penetrate below layers of lava flows, hence the observed sediment thickness cannot be reliably taken as the maximum thickness of the basin fill. Supporting this is the maximum depth of the lake; it is 480 m, indicating that considerable accommodation space has been created. Secondly, the surface lake level of Kivu is some 600 m higher than the adjacent lake levels to the north (Lake George) and south (Lake Tanganyika). This is clearly a large-scale effect, possibly related to a magmatic/heat flow effect with a ~150 km diameter. The buoyancy of the region would have had a considerable effect on subsidence so that Lake Kivu could not be simply compared with Lake Albert.

[32] The numerical modeling results show furthermore that decompressional melting as a result of passive mantle

upwelling beneath the rift zone is not predicted at the early stages of extension (as in western branch) with normal mantle temperatures. Previous studies show that melts are generated by decompression melting during rifting when the crust is thinned with a factor >2 [*McKenzie and Bickle*, 1988], unless mantle temperatures have been elevated considerably during rifting, or increased mantle upwelling (small-scale convection) occurs, for example, along a craton-noncraton boundary [*King and Anderson*, 1998; *Pascal et al.*, 2002]. In these cases, pressure release melting may start almost immediately upon extension of the lithosphere [*McKenzie and Bickle*, 1988], giving rise to the sparse magmatism in the western branch. This volcanic activity seems to concentrate in the accommodation zones, not in the sedimentary basins, while the basins and not the accommodation zones would be the preferred location for generating pressure release melting in the numerical models. Why would this magma erupt in the accommodation zones instead of in the basins?

[33] The presence of early volcanism raises the question: Is the deformation "predetermined" i.e., the volcanism controls rift development and the location of accommodation zones, or is it controlled as the rift develops by rift structures such as transfer zones? The above analogue modeling results support that the main rift architecture is controlled by the trend of mobile belts, and thus accommodation zone location may not be controlled by magmatic processes. Structural studies in lakes George and Edward region [*Lærdal and Talbot*, 2002] support that accommodation zones are controlled by WNW to NW trending basement lineaments interfering with the NNE to NE trend of the Miocene rifting; reactivation of these transversal Precambrian fabrics and their intersections with the rift faults control the eruption of the early magmas. Further accumulation of magma at transfer zones may be enhanced by rift-orthogonal magma migration [e.g., *Corti et al.*, 2003, 2004], and its ascent facilitated by the deeply penetrating transfer faults [e.g., *Ebinger et al.*, 1989]. In turn, magma emplacement may contribute to the final architecture of the accommodation zones by locally controlling the deformation style (intrusion versus brittle faulting): The magmatic areas lack large border faults; they die out approaching the magmatic centers, consequently brittle extension does not appear to be transferred onto other faults, hence either extension dies out, or it is transferred to igneous intrusions.

[34] Thus migration of the scarce magma volumes related to anomalous mantle temperatures at the early stages of extension (as in western branch) may be controlled by intersecting high-angle structural trends, causing eruption at accommodation zones. Increasing amount of lithospheric extension will conversely result in decompressional melting below the main sedimentary basins and pronounced magmatic segmentation of the rift, as predicted by the models. Similar evolution has been speculated on the basis of structural investigations for the volcanic craters in the Toro-Ankole and Virunga volcanic provinces, whose trend is aligned parallel to the structural feature that was dominating in the area at the time of volcanic initiation [*Lærdal and Talbot*, 2002]. For the older volcanic province (Virunga),

the dominant structure at the time of initiation was the Precambrian basement lineaments, while the dominant structure during initiation of the Toro-Ankole volcanic province was the NNE-SSW oriented Miocene rift [*Lærdal and Talbot*, 2002].

5. Conclusions

[35] As early as several decades ago it has been suggested that the tectonic inheritance has controlled the location and development the western branch of the East African Rift [e.g., *McConnell*, 1969]. The relationship between rifting and pre-existing weaknesses is indeed obvious on a continental scale, as normal faults localize within the mobile belts at the craton's western edge. However, the more closely we look at single basins or fault systems the more the picture of the relations between structure and inheritance becomes complex and this has complicated the assessment of the role of preexisting structures on rift architecture. The current analogue and numerical models shed new light on this old problem by considering in detail the role of discrete upper crustal fabrics and lithospheric weakness zones on the rift structure.

[36] First-order segmentation characteristics of the EAR are shown by the above described experiments to be controlled by the geometry of the weak, Proterozoic mobile belts at the western border of the Tanzanian craton. Model results illustrate that on a regional-scale rift localization at the curved craton's border results in an arcuate rift system, which implies that under a constant extensional stress field, part of the western branch experienced orthogonal extension and part oblique or highly oblique extension. This varying extension direction along the rift zone results in lengthwise varying rift asymmetry, segmentation characteristics and border fault architecture (trend, length and kinematics). As predicted by the finite element modeling the rifts oblique to the regional extension direction (lakes Rukwa and Albert) appear to display lower amounts of basin subsidence and extension, than the more extension-orthogonal Lake Tanganyika. In both Lake Rukwa and Lake Albert, there is some controversy about the thickness of the Cenozoic section and actually how much is of Mesozoic age. The modeling here supports the interpretations of thinner Cenozoic section. Part of the preexisting fabric associated with the oblique rifts appears to be older brittle Late Paleozoic-Mesozoic extensional rift systems that themselves were influenced by the Precambrian basement fabrics.

[37] Another oblique rift trend, Lake Kivu, does not fit so easily into the assessment because of the overprint of uplift and extrusive activity associated with an important magmatic province. However, the emplacement of magma early in the rift evolution was focused on a region where Precambrian basement structures meet at a high angle with the brittle rift structures. These intersecting trends probably focused magmatic activity which in turn, early in the rift history, then influenced the location of the accommodation zones by transferring upper crustal extension from predominantly brittle faulting to predominantly tensile failure accommodating igneous intrusions.

[38] Superpositioned is the influence of inherited discrete fabrics and reactivated structures, which control local fault geometries and architecture of accommodation zones. For example, when lithospheric material in the weak zone is substantially weaker than the surrounding strong plate, stresses rotate between these materials, and multiple areas of localization that are somewhat rotated with respect to the orientation of the weak zone, are formed. In this way, seemingly enigmatic correlations between preexisting fabrics and basin structures can be explained. Inherited weakness reactivation is thus able to account for the dominant structural framework of the western branch; other parameters such as magmatic diapirs or changes in stress field during rifting may have controlled structures at a more local scale.

References

Bellahsen, N., and J. M. Daniel (2005), Fault reactivation control on normal fault growth: An experimental study, *J. Struct. Geol.*, *27*, 769–780.

Benoit, M. H., A. A. Nyblade, and J. C. VanDecar (2006), Upper mantle P-wave speed variations beneath Ethiopia and the origin of the Afar hotspot, *Geology*, *34*, 329–332.

Bungum, H., and A. A. Nnko (1984), Seismicity and tectonics of the Steigler's George area, Tanzania, *J. Geophys. Res.*, *89*, 1874–1888.

Calais, E., C. Ebinger, C. Hartnady, and J. M. Nocquet (2006), Kinematics of the East African Rift from GPS and earthquake vector data, in *The Afar Volcanic Province Within the East African Rift System*, edited by G. Yirgu, C. J. Ebinger, and P. K. H. Maguire, *Geol. Soc. Spec. Publ.*, *253*, 9–22.

Camelbeeck, T., and M. D. Iranga (1996), Deep crustal earthquakes and active faults along the Rukwa Trough, eastern Africa, *Geophys. J. Int.*, *124*, 612–630.

Chorowitz, J. (2005), The East African Rift system, *J. Afr. Earth Sci.*, *43*, 379–410.

Corti, G., M. Bonini, S. Conticelli, F. Innocenti, P. Manetti, and D. Sokoutis (2003), Analogue modelling of continental extension: A review focused on the relations between the patterns of deformation and the presence of magma, *Earth Sci. Rev.*, *63*, 169–247.

Corti, G., M. Bonini, D. Sokoutis, F. Innocenti, P. Manetti, S. Cloetingh, and G. Mulugeta (2004), Continental rift architecture and patterns of magma migration: A dynamic analysis based on centrifuge models, *Tectonics*, *23*, TC2012, doi:10.1029/2003TC001561.

Daly, M. C., J. Chorowitz, and J. D. Fairhead (1989), Rift basin evolution in Africa: The influence of reactivated steep basement shear zones, in *Inversion Tectonics*, edited by M. A. Cooper and G. D. Williams, *Geol. Soc. Spec. Publ.*, *44*, 309–334.

Degens, E. T., R. P. von Herzen, H. K. Wong, W. G. Deuser, and H. W. Jannasch (1973), Lake Kivu: Structure, chemistry and biology of an East African Rift lake, *Int. J. Earth Sci.*, *62*, 245–277.

Delvaux, D. (2001), Karoo rifting in western Tanzania: Precursor of Gondwana breakup?, in *Contributions to Geology and Paleontology of Gondwana. In Honour of Prof. Dr. Helmut Wopfner*, edited by R. H. Weiss, pp. 111–125, Geol. Inst., Univ. of Cologne, Cologne, Germany.

Delvaux, D., K. Levi, R. Kajara, and J. Sorata (1992), Cenozoic paleostress and kinematic evolution of the Rukwa, North Malawi rift valley (East African System), *Bull. Cent. Rech. Explor. Prod. Elf Aquitaine*, *16*, 383–406.

Ebinger, C. J. (1989), Tectonic development of the western branch of the East African Rift system, *Geol. Soc. Am. Bull.*, *101*, 885–903.

Ebinger, C. J., and N. H. Sleep (1998), Cenozoic magmatism throughout east Africa resulting from impact of a single plume, *Nature*, *395*, 788–791.

Ebinger, C. J., B. Rosendahl, and D. Reynolds (1987), Tectonic model of the Malawi Rift, Africa, *Tectonophysics*, *141*, 215–235.

Ebinger, C. J., A. L. Deino, R. E. Drake, and A. L. Tesha (1989), Chronology of volcanism and rift basin propagation: Rungwe volcanic province, East Africa, *J. Geophys. Res.*, *94*, 15,785–15,803.

Fairhead, J. D., and G. W. Stuart (1982), The seismicity of the East African Rift system and comparison with other continental rifts, in *Continental and Oceanic Rifts*, *Geophys. Monogr. Ser.*, vol. 8, edited by G. Palmason, pp. 41–61, AGU, Washington, D. C.

Fernandes, R. M. S., B. A. C. Ambrosius, R. Noomed, L. Bastos, J. Combinck, J. M. Miranda, and W. Spakman (2004), Angular velocities of Nubia and Somalia from continuous GPS data: Implications on present-day relative kinematics, *Earth Planet. Sci. Lett.*, *222*, 197–208.

Foster, A. N., and J. A. Jackson (1998), Source parameters of large African earthquakes: Implications for crustal rheology and regional kinematics, *Geophys. J. Int.*, *134*, 422–448.

Furlong, K. P., S. D. Sheaffer, and R. Malservisi (2001), Thermal rheological controls on deformation within oceanic transforms, in *The Nature and Tectonic Significance of Fault Zone Weakening*, edited by R. E. Holdsworth et al., *Geol. Soc. Spec. Publ.*, *186*, 65–83.

George, R., N. Rogers, and S. Kelley (1998), Earliest magmatism in Ethiopia: Evidence for two mantle plumes in one flood basalt province, *Geology*, *26*, 923–926.

Govers, R., and M. J. R. Wortel (2005), Lithosphere tearing at STEP faults: Response to edges of subduction zones, *Earth Planet. Sci. Lett.*, *236*, 505–523.

Greenough, C., and K. R. Robinson (2000), The finite element library, release 4.0, Rutherford Appleton Lab., Didicot, U.K. (Available at http://www.softeng.cse.clrc.ac.uk)

Jackson, J., and T. Blenkinsop (1993), The Malawi earthquake of 10 March 1989: Deep faulting within the East African Rift system, *Tectonics*, *12*, 1131–1139.

Jestin, F., P. Huchon, and M. Gaulier (1984), The Somalia plate and the East African Rift system: Present-day kinematics, *Geophys. J. Int.*, *116*, 637–654.

Karner, G. D., B. R. Byamungu, C. J. Ebinger, A. B. Kampunzu, R. A. Mukasa, J. Nyakaana, E. N. T. Rubondo, and N. M. Upcott (2000), Distribution of crustal extension and regional basin architecture of the Albertine rift system, East Africa, *Mar. Pet. Geol.*, *17*, 1131–1150.

Kebede, F., and O. Kulhanek (1991), Recent seismicity of the East African Rift system and its implications, *Phys. Earth. Planet. Inter.*, *68*, 259–273.

King, S. D., and D. L. Anderson (1998), Edge-driven convection, *Earth Planet. Sci. Lett.*, *160*, 289–296.

Kirby, S. H., and A. K. Kronenberg (1987), Rheology of the lithosphere: Selected topics, *Rev. Geophys.*, *25*, 1219–1244.

Krause, D. W., M. D. Gottfried, P. M. O'Connor, and E. M. Roberts (2003), A Cretaceous mammal from Tanzania, *Acta Palaeontol. Polonica*, *48*, 321–330.

Kusznir, N. J., A. M. Roberts, and C. K. Morley (1995), Forward and reverse modeling of rift basin formation, in *Volcanism Associated With Extension at Consuming Plate Margins*, edited by J. L. Smellie, *Geol. Soc. Spec. Publ.*, *80*, 33–56.

Lærdal, T., and M. R. Talbot (2002), Basin neotectonics of lakes Edward and Georgem, East African Rift, *Palaeogeogr. Palaeoclimatol. Palaeoecol.*, *187*, 213–232.

Lemaux, J., R. Gordon, and J.-Y. Royer (2002), location of the Nubia-Somalia boundary along the Southwest Indian Ridge, *Geology*, *30*, 339–342.

Le Turdu, C., J. J. Tiercelin, J. P. Richert, J. Rolet, J. P. Xavier, R. W. Renaut, K. E. Lezzar, and C. Coussement (1999), Influence of pre-existing oblique discontinuities on the geometry and evolution of extensional fault patterns: Evidence from the Kenya Rift using SPOT imagery, in *Geoscience of Rift Systems—Evolution of East Africa*, edited by C. K. Morley, *AAPG Stud. Geol.*, *44, 173–191.*

Lezzar, K. E., J.-J. Tiercelin, C. Le Turdu, A. S. Cohen, D. J. Reynolds, B. Le Gall, and C. A. Scholz (2002), Control of normal fault interaction on the distribution of major Neogene sedimentary depocenters, Lake Tanganyika, East African Rift, *AAPG Bull.*, *86*, 1027–1059.

McConnell, R. B. (1969), The East African Rift system, *Nature*, *215*, 578–581.

McConnell, R. (1972), Geological development of the rift system of East Africa, *Geol. Soc. Am. Bull.*, *83*, 2549–2572.

McKenzie, D. P., and M. J. Bickle (1988), The volume and composition of melt generated by extension of the lithosphere, *J. Petrol.*, *29*, 625–679.

Melosh, H. J., and A. Raefsky (1980), The dynamical origin of subduction zone topography, *Geophys. J. R. Astron. Soc.*, *60*, 333–354.

Michon, L., and D. Sokoutis (2005), Interaction between structural inheritance and extension direction during graben and depocentre formation: An experimental approach, *Tectonophysics*, *409*, 125–146.

Morley, C. K. (1988), Variable extension in Lake Tanganyika, *Tectonics*, *7*, 785–801.

Morley, C. K. (1989), Extension, detachments and sedimentation in continental rifts (with particular reference to East Africa), *Tectonics*, *8*, 1175–1192.

Morley, C. K. (1999a), Influence of pre-existing fabrics on rift structure, in *Geoscience of Rift Systems—Evolution of East Africa*, edited by C. K. Morley, *AAPG Stud. Geol.*, *44*, 151–160.

Morley, C. K. (1999b), How successful are analog models in addressing the influence of pre-existing fabrics on rift structure?, *J. Struct. Geol.*, *21*, 1267–1274.

Morley, C. K., R. A. Nelson, T. L. Patton, and S. G. Munn (1990), Transfer zones in the East African Rift system and their relevance to hydrocarbon exploration in rifts, *AAPG Bull.*, *74*, 1234–1253.

Morley, C. K., S. M. Cunningam, W. A. Wescott, and R. M. Harper (1999), Geology and geophysics of the Rukwa Rift, in *Geoscience of Rift Systems—Evolution of East Africa*, edited by C. K. Morley, *AAPG Stud. Geol.*, *44*, 91–110.

Nyblade, A. A., and R. A. Brazier (2002), Precambrian lithospheric controls on the development of the East African Rift system, *Geology*, *30*, 755–758.

Nyblade, A. A., and C. A. Langston (1995), East African earthquakes below 20 km depth and their implications for crustal structure, *Geophys. J. Int.*, *121*, 49–62.

O'Connor, P. M., M. D. Gottfried, N. J. Stevens, E. M. Roberts, S. Ngasala, S. Kapilima, and R. Chami (2006), A new vertebrate fauna from the Cretaceous Red Sandstone Group, Rukwa Rift Basin, southwestern Tanzania, *J. Afr. Earth Sci.*, *44*, 277–288.

Pascal, C., J. W. van Wijk, S. A. P. L. Cloetingh, and G. R. Davies (2002), Effect of lithosphere thickness heterogeneities in controlling rift localization: Numerical modeling of the Oslo Graben, *Geophys. Res. Lett.*, *29*(9), 1355, doi:10.1029/2001GL014354.

Petit, C., and C. Ebinger (2000), Flexure and mechanical behavior of cratonic lithosphere: Gravity models of the East African and Baikal rifts, *J. Geophys. Res.*, *105*, 19,151–19,162.

Ring, U. (1994), The influence of preexisting structure on the evolution of the Cenozoic Malawi Rift (East African Rift system), *Tectonics*, *13*, 313–326.

Ring, U., C. Betzler, and D. Delvaux (1992), Normal vs. strike-slip faulting during rift development in East Africa: The Malawi rift, *Geology*, *20*, 1015–1018.

Roberts, E. M., P. M. O'Connor, M. D. Gottfried, N. J. Stevens, S. Kapilima, and S. Nasala (2004), Revised stratigraphy and age of the Red Sandstone Group in the Rukwa Rift Basin, Tanzania, *Cretaceous Res.*, *25*, 749–759.

Rosendahl, B. R. (1987), Architecture of continental rifts with special reference to East Africa, *Annu. Rev. Earth Planet. Sci.*, *15*, 445–503.

Rosendahl, B., D. Reynolds, P. Lorber, C. Burgess, J. McGill, D. Scott, J. Lambiase, and S. Derksen (1986), Structural expressions of rifting: Lessons from Lake Tanganyika, in *Sedimentation in the African Rifts*, edited by L. E. Frostick et al., *Geol. Soc. Spec. Publ.*, *25*, 29–43.

Rosendahl, B. R., E. Kilembe, and K. Kaczmarick (1992), Comparison of the Tanganyika, Malawi, Rukwa, and Turkana rift zones from analyses of seismic reflection data, *Tectonophysics*, *213*, 235–256.

Scholz, C. H., and J. C. Contreras (1998), Mechanics of continental rift architecture, *Geology*, *26*, 967–970.

Shudofsky, G. N. (1985), Source mechanisms and focal depths of East African earthquakes using Raleigh-wave inversion and body-wave modelling, *Geophys. J. R. Astron. Soc.*, *83*, 563–614.

Shudofsky, G. N., S. Cloetingh, S. Stein, and R. Wortel (1987), Unusually deep earthquakes in East Africa: Constraints on the thermo-mechanical structure of a continental rift system, *Geophys. Res. Lett.*, *14*, 741–744.

Tron, V., and J. P. Brun (1991), Experiments on oblique rifting in brittle-ductile systems, *Tectonophysics*, *188*, 71–84.

Tsenn, M. C., and N. L. Carter (1987), Upper limits of power law creep of rocks, *Tectonophysics*, *136*, 1–26.

Turcotte, G. L., and D. Schubert (2002), *Geodynamics*, 2nd ed., 456 pp., Cambridge Univ. Press, New York.

van Wijk, J. W. (2005), Role of weak zone orientation in continental lithosphere extension, *Geophys. Res. Lett.*, *32*, L02303, doi:10.1029/2004GL022192.

van Wijk, J. W., and D. K. Blackman (2005), Deformation of oceanic lithosphere near slow-spreading ridge discontinuities, *Tectonophysics*, *407*, 211–225.

van Wijk, J. W., and D. K. Blackman (2007), Development of en-echelon magmatic segments along oblique spreading ridges, *Geology*, *35*(7), 599–602, doi:10.1130/G23294A.1.

Versfelt, J., and B. R. Rosendahl (1989), Relationships between pre-rift structure and rift architecture in lakes Tanganyika and Malawi: East Africa, *Nature*, *337*, 354–357.

Walker, K. T., A. A. Nyblade, S. L. Klemperer, G. H. R. Bokelmann, and T. J. Owens (2004), On the relationship between extension and anisotropy: Constraints from shear wave splitting across the East African Plateau, *J. Geophys. Res.*, *109*, B08302, doi:10.1029/2003JB002866.

Yale, D. P., J. M. Rodriguez, T. B. Mercer, and D. W. Blaisdell (1994), In-situ stress orientation and the effects of local structure—Scott Field, North Sea, paper presented at the 1994 Eurorock Conference, Los Alamos Natl. Lab., Delft, Netherlands.

————————

S. Cloetingh, Tectonics Department, Vrije Universiteit, De Boelelaan 1085, NL-1081 HV Amsterdam, Netherlands. (sierd.cloetingh@falw.vu.nl)

G. Corti, CNR-Istituto di Geoscienze e Georisorse, Unità Operativa di Firenze, Via G. La Pira, 4, I-50121, Florence, Italy. (giacomo.corti@unifi.it)

C. K. Morley, PTT Exploration and Production, 555 Vibhavadi-Rangsit Road, Chatuchak, Bangkok, Thailand. (christopherk@pttep.com)

J. van Wijk, Earth and Environmental Sciences Division, Los Alamos National Laboratory, Los Alamos, NM 87545, USA. (jolante@lanl.gov)